ISSN 0965-5425, Computational Mathematics and Mathematical Physics, 2015, Vol. 55, No. 11, pp. 1899–1912. © Pleiades Publishing, Ltd., 2015.

Effects of Partial Slip on the Peristaltic Transport of a Hyperbolic Tangent Fluid Model in an Asymmetric Channel[1]

S. Akram[a]* and S. Nadeem[b]

[a] *Department of Basic Sciences, MCS, National University of Sciences and Technology (NUST), Islamabad Pakistan*

[b] *Department of Mathematics, Quaid-i-Azam University 45320, Islamabad 44000 Pakistan*

**e-mail: drsafiaakram@gmail.com; safia_akram@yahoomail.com*

Received February 20, 2014: in final form, April 14, 2014

Abstract—In the present analysis, we have modeled the governing equations of two dimensional hyperbolic tangent fluid model under the assumptions of long wavelength and low Reynolds number. The flow is investigated in a wave frame of reference moving with the velocity of the wave. The governing equations of hyperbolic tangent fluid have been solved using regular perturbation method. The expression for pressure rise has been calculated using numerical integrations. The behavior of different physical parameters have been discussed graphically.

DOI: 10.1134/S0965542515110147

Keywords: modeling of hyperbolic tangent fluid model, asymmetric channel, analytical solutions, partial slip-condition.

1. INTRODUCTION

Various applications of peristaltic flows in physiology and industry have produced interest among the researchers [1–8]. Such application include urine transport from kidney to bladder, through ureter, the movement of chyme in the gastrointestinal tract, the movement of spermatozoa in the human reproductive tract and the vasomotion of small blood vessels etc. The theoretical idea of peristaltic mechanism was given by Shapiro [9] which was latter on experimentally tested by Latham [10]. After Latham a large amount of studies have presented on the peristaltic phenomena [11–16].

In the references cited above [1–16] no slip condition has been taken into account. However, in certain situations standard no slip is not applicable. Recently, Hayat et al. [17] discussed the slip effects on the peristaltic motion of a viscous fluid through a porous medium in an asymmetric channel. Ebaid [18] discussed the problem of Hayat et al. [17] incorporating the effects of MHD in the place of porous medium term. Only a few papers are available in literature in which the effects of partial slip on the peristaltic motion of non-Newtonian fluids have been taken. In non-Newtonian fluids in the presence of the slip conditions the governing equations and boundary conditions are highly non-linear and complicated. The influence of slip on the peristaltic motion of a third order fluid in an asymmetric channel has been discussed by Hayat et al. [19]. Nadeem and Akram [20] have discussed the peristaltic motion of a Jeffrey fluid in an asymmetric channel with partial slip conditions. The aim of the present paper is to discuss the effects of the slip condition on the peristaltic flow of a tangent hyperbolic fluid model. To the best of authors knowledge no attempt has been made to discussed the slip effects of tangent hyperbolic fluid model. The governing highly non linear differential equations and boundary conditions are simplified using the assumptions of long wave length and low Reynolds number. The reduced equations are then solved analytically by a well known perturbation technique. The expression of pressure rise has been computed numerically using mathematics software. The results are discussed through graphs for various physical parameters of the proposed problem.

2. MATHEMATICAL FORMULATION

For an incompressible fluid the balance of mass and momentum are given by

$$\operatorname{div}\mathbf{V} = 0, \tag{1}$$

[1] The article is published in the original.

$$\rho\frac{d\mathbf{V}}{dt} = \operatorname{div}\mathbf{S} + \rho\mathbf{f}, \tag{2}$$

where ρ is the density, $\mathbf{V}$ is the velocity vector, $\mathbf{S}$ is the Cauchy stress tensor, $\mathbf{f}$ represents the specific body force and d/dt represents the material time derivative. The constitutive equation for hyperbolic tangent fluid is given by [21, 22]

$$\mathbf{S} = -P\mathbf{I} + \tau, \tag{3}$$

$$\bar{\boldsymbol{\tau}} = -[[\eta_\infty + (\eta_0 + \eta_\infty)\tanh(\Gamma\bar{\dot{\gamma}})^n]\bar{\dot{\gamma}}], \tag{4}$$

in which $-P\mathbf{I}$ is the spherical part of the stress due to the constraint of incompressibility, $\boldsymbol{\tau}$ is the extra stress tensor, η_∞ is the infinite shear rate viscosity, η_0 is the zero shear rate viscosity, Γ is the time constant, n is the power law index and $\bar{\dot{\gamma}}$ is defined as

$$\bar{\dot{\gamma}} = \sqrt{\frac{1}{2}\sum_i\sum_j \bar{\dot{\gamma}}_{ij}\bar{\dot{\gamma}}_{ji}} = \sqrt{\frac{1}{2}\Pi}. \tag{5}$$

Here, Π is the second invariant strain tensor. We consider the constitutive Eq. (4) for the case in which $\eta_\infty = 0$ and $\Gamma\bar{\dot{\gamma}} < 1$. The component of extra stress tensor therefore, can be written as

$$\bar{\boldsymbol{\tau}} = -\eta_0[(\Gamma\bar{\dot{\gamma}})^n]\bar{\dot{\gamma}} = -\eta_0[(1+\Gamma\bar{\dot{\gamma}}-1)^n]\bar{\dot{\gamma}} = -\eta_0[1+n(\Gamma\bar{\dot{\gamma}}-1)]\bar{\dot{\gamma}}. \tag{6}$$

Let us consider the peristaltic transport of an incompressible hyperbolic tangent fluid in a two dimensional channel of the width $\bar{d}_1 + \bar{d}_2$. The flow is generated by the sinusoidal wave trains propagating with the constant speed c along the channel walls. The geometry of the wall surface is defined as

$$\begin{aligned} Y = H_1 &= \bar{d}_1 + \bar{a}_1\cos\left[\frac{2\pi}{\lambda}(\bar{X}-c\bar{t})\right], \\ Y = H_2 &= -\bar{d}_2 - \bar{b}_1\cos\left[\frac{2\pi}{\lambda}(\bar{X}-c\bar{t})+\phi\right], \end{aligned} \tag{7}$$

where $\bar{a}_1$ and $\bar{b}_1$ are the amplitudes of the waves, λ is the wave length, $\bar{d}_1 + \bar{d}_2$ is the width of the channel, c is the velocity of propagation, $\bar{t}$ is the time and $\bar{X}$ is the direction of wave propagation. The phase difference ϕ varies in the range $0 \le \phi \le \pi$ in which $\phi = 0$ corresponds to symmetric channel and the waves out of phase and $\phi = \pi$, the waves are in phase, further, $\bar{a}_1$, $\bar{b}_1$, $\bar{d}_1$, $\bar{d}_2$ and ϕ satisfies the condition

$$\bar{a}_1^2 + \bar{b}_1^2 + 2\bar{a}_1\bar{b}_1\cos\phi \le (\bar{d}_1 + \bar{d}_2)^2.$$

The equations governing the flow of a tangent hyperbolic fluid are given by

$$\frac{\partial\bar{U}}{\partial\bar{X}} + \frac{\partial\bar{V}}{\partial\bar{Y}} = 0, \tag{8}$$

$$\rho\left(\frac{\partial\bar{U}}{\partial\bar{t}} + \bar{U}\frac{\partial\bar{U}}{\partial\bar{X}} + \bar{V}\frac{\partial\bar{U}}{\partial\bar{Y}}\right) = -\frac{\partial\bar{P}}{\partial\bar{X}} - \frac{\partial\bar{\tau}_{\bar{X}\bar{X}}}{\partial\bar{X}} - \frac{\partial\bar{\tau}_{\bar{X}\bar{Y}}}{\partial\bar{Y}}, \tag{9}$$

$$\rho\left(\frac{\partial\bar{V}}{\partial\bar{t}} + \bar{U}\frac{\partial\bar{V}}{\partial\bar{X}} + \bar{V}\frac{\partial\bar{V}}{\partial\bar{Y}}\right) = -\frac{\partial\bar{P}}{\partial\bar{Y}} - \frac{\partial\bar{\tau}_{\bar{X}\bar{Y}}}{\partial\bar{X}} - \frac{\partial\bar{\tau}_{\bar{Y}\bar{Y}}}{\partial\bar{Y}}. \tag{10}$$

Since flow in laboratory and wave frames are treated unsteady and steady, respectively. The two frames are related by the transformations

$$\bar{x} = \bar{X} - c\bar{t}, \quad \bar{y} = \bar{Y}, \quad \bar{u} = \bar{U} - c, \quad \bar{v} = \bar{V} \quad \text{and} \quad \bar{p}(x) = \bar{P}(X,t). \tag{11}$$

Introducing the following non-dimensional quantities

$$x = \frac{\bar{x}}{\lambda}, \quad y = \frac{\bar{y}}{d_1}, \quad u = \frac{\bar{u}}{c}, \quad t = \frac{c}{\lambda}\bar{t}, \quad h_1 = \frac{\bar{h}_1}{\bar{d}_1}, \quad h_2 = \frac{\bar{h}_2}{\bar{d}_1}, \quad \tau_{xx} = \frac{\lambda}{\eta_0 c}\bar{\tau}_{\bar{x}\bar{x}}, \quad \tau_{xy} = \frac{\bar{d}_1}{\eta_0 c}\bar{\tau}_{\bar{x}\bar{y}},$$
$$\tau_{yy} = \frac{\bar{d}_1}{\eta_0 c}\bar{\tau}_{\bar{y}\bar{y}}, \quad \delta = \frac{\bar{d}_1}{\lambda}, \quad \mathrm{Re} = \frac{\rho c \bar{d}_1}{\eta_0}, \quad We = \frac{\Gamma c}{d_1}, \quad P = \frac{\bar{d}_1^2}{c\lambda\eta_0}\bar{p}, \quad \dot{\gamma} = \frac{\bar{\dot{\gamma}}\bar{d}_1}{c}. \tag{12}$$

Using Eqs. (11), (12) and values of stream function $\Psi(u = \frac{\partial \Psi}{\partial y}, v = -\frac{\partial \Psi}{\partial x})$, the continuity equation (8) is identically satisfied and Eqs. (9) and (10) takes the following form

$$\delta \mathrm{Re}\left[\left(\frac{\partial \Psi}{\partial y}\frac{\partial}{\partial x} - \frac{\partial \Psi}{\partial x}\frac{\partial}{\partial y}\right)\frac{\partial \Psi}{\partial y}\right] = -\frac{\partial P}{\partial x} - \delta^2\frac{\partial \tau_{xx}}{\partial x} - \frac{\partial \tau_{xy}}{\partial y}, \tag{13}$$

$$\delta^3 \mathrm{Re}\left[\left(\frac{\partial \Psi}{\partial y}\frac{\partial}{\partial x} - \frac{\partial \Psi}{\partial x}\frac{\partial}{\partial y}\right)\frac{\partial \Psi}{\partial x}\right] = -\frac{\partial P}{\partial y} - \delta^2\frac{\partial \tau_{xy}}{\partial x} - \delta\frac{\partial \tau_{yy}}{\partial y}, \tag{14}$$

where

$$\tau_{xx} = -2[1 + n(We\dot{\gamma} - 1)]\frac{\partial^2 \Psi}{\partial x \partial y},$$

$$\tau_{xy} = -[1 + n(We\dot{\gamma} - 1)]\left(\frac{\partial^2 \Psi}{\partial y^2} - \delta^2\frac{\partial^2 \Psi}{\partial x^2}\right),$$

$$\tau_{yy} = 2\delta[1 + n(We\dot{\gamma} - 1)]\frac{\partial^2 \Psi}{\partial x \partial y},$$

$$\dot{\gamma} = \left[2\delta^2\left(\frac{\partial^2 \Psi}{\partial x \partial y}\right)^2 + \left(\frac{\partial^2 \Psi}{\partial y^2} - \delta^2\frac{\partial^2 \Psi}{\partial x^2}\right)^2 + 2\delta^2\left(\frac{\partial^2 \Psi}{\partial x \partial y}\right)^2\right]^{1/2},$$

in which δ is the wave, Re represents the Reynolds number and *We* represent the Weissenberg numbers.

For long wavelength approximation [22] Eqs. (13) and (14) reduce in the following form

$$\frac{\partial P}{\partial x} = \frac{\partial}{\partial y}\left[1 + n\left(We\frac{\partial^2 \Psi}{\partial y^2} - 1\right)\right]\frac{\partial^2 \Psi}{\partial y^2}, \tag{15}$$

$$\frac{\partial P}{\partial y} = 0. \tag{16}$$

Elimination of pressure from Eqs. (15) and (16) yield

$$\frac{\partial^2}{\partial y^2}\left[1 + n\left(We\frac{\partial^2 \Psi}{\partial y^2} - 1\right)\right]\frac{\partial^2 \Psi}{\partial y^2} = 0. \tag{17}$$

The instantaneous volume flow rate in the fixed frame is defined as

$$Q = \int_{\bar{H}_2}^{\bar{H}_1} \bar{U}(\bar{X}, \bar{Y}, \bar{t})d\bar{Y}. \tag{18}$$

In the wave frame the rate of the volume flow is defined as

$$q = \int_{\bar{h}_1}^{\bar{h}_2} u(\bar{x}, \bar{y})d\bar{y}, \tag{19}$$

in which $\bar{h}_1$ and $\bar{h}_2$ are the functions of x only. Prom Eq. (11), (18) and (19) we obtain

$$Q = q + c\bar{h}_1(\bar{x}) - c\bar{h}_2(\bar{x}). \tag{20}$$

The time mean flow over a period T at a fixed position $\bar{X}$ is defined as

$$\bar{Q} = \frac{1}{T}\int_0^T Q dt. \tag{21}$$

Making use of (20) into (21), and after integrating, we get

$$\bar{Q} = q + cd_1 - cd_2, \tag{22}$$

The dimensionless time-mean flows Q in the laboratory frame and F in the wave frame are defined as

$$Q = \frac{\bar{Q}}{cd_1}, \quad F = \frac{q}{cd_1}. \tag{23}$$

Therefore Eq. (22) can be written as

$$Q = F + 1 + d, \tag{24}$$

The boundary conditions in terms of stream function Ψ are defined as

$$\begin{aligned} \Psi &= \frac{F}{2}, \quad \frac{\partial \Psi}{\partial y} = -\beta\tau_{xy} - 1 \quad \text{for } y = h_1(x), \\ \Psi &= -\frac{F}{2}, \quad \frac{\partial \Psi}{\partial y} = \beta\tau_{xy} - 1 \quad \text{for } y = h_2(x), \end{aligned} \tag{25}$$

where a, b, ϕ and d satisfy the following relation

$$a^2 + b^2 + 2ab\cos\phi \le (1+d)^2.$$

3. PERTURBATION SOLUTION

For the perturbation solution, we expand Ψ, F and P as

$$\Psi = \Psi_0 + We\Psi_1 + O(We^2), \tag{26}$$

$$F = F_0 + WeF_1 + O(We^2), \tag{27}$$

$$P = P_0 + WeP_1 + O(We^2). \tag{28}$$

Substituting above expressions in Eqs. (15), (17) and (25), collecting the powers of We, we, obtain the following systems

3.1. System of Order We^0

$$\frac{\partial^4 \Psi_0}{\partial y^4} = 0, \tag{29}$$

$$\frac{\partial P_0}{\partial x} = (1-n)\frac{\partial^3 \Psi_0}{\partial y^3}, \tag{30}$$

$$\Psi_0 = \frac{F_0}{2}, \quad \frac{\partial \Psi_0}{\partial y} = \beta\left((1-n)\frac{\partial^2 \Psi_0}{\partial y^2}\right) - 1 \quad \text{at } y = h_1(x), \tag{31}$$

$$\Psi_0 = -\frac{F_0}{2}, \quad \frac{\partial \Psi_0}{\partial y} = -\beta\left((1-n)\frac{\partial^2 \Psi_0}{\partial y^2}\right) - 1 \quad \text{at } y = h_2(x). \tag{32}$$

3.2. System of Order We[1]

$$\frac{\partial^4 \Psi_1}{\partial y^4} = \frac{n}{n-1}\frac{\partial^2}{\partial y^2}\left(\frac{\partial^2 \Psi_0}{\partial y^2}\right)^2, \tag{33}$$

$$\frac{\partial P_1}{\partial x} = (1-n)\frac{\partial^3 \Psi_1}{\partial y^3} + n\frac{\partial}{\partial y}\left(\frac{\partial^2 \Psi_0}{\partial y^2}\right)^2, \tag{34}$$

$$\Psi_1 = \frac{F_1}{2}, \quad \frac{\partial \Psi_1}{\partial y} = \beta\left((1-n)\frac{\partial^2 \Psi_1}{\partial y^2} + n\left(\frac{\partial^2 \Psi_0}{\partial y^2}\right)^2\right) \quad \text{at } y = h_1(x), \tag{35}$$

$$\Psi_1 = -\frac{F_1}{2}, \quad \frac{\partial \Psi_1}{\partial y} = -\beta\left((1-n)\frac{\partial^2 \Psi_1}{\partial y^2} + n\left(\frac{\partial^2 \Psi_0}{\partial y^2}\right)^2\right) \quad \text{at } y = h_2(x). \tag{36}$$

3.3. Solution for System of Order We[0]

Solution of Eq. (29) satisfying the boundary conditions (31) and (32) can be written as

$$\begin{aligned}\psi_0 = {} & \frac{-1}{2(h_1-h_2)^2(-6A+h_1-h_2)}(-6AF_0(h_1^2-h_2^2) + F_0(h_1^3+h_2^3) - 3F_0h_1h_2(h_1+h_2) - 2h_1h_2(h_1^2+h_2^2)) \\ & + \frac{6(F_0+h_1-h_2)(h_1+h_2)}{(h_1-h_2)^2(-6A+h_1-h_2)}\frac{y^2}{2!} + \frac{-1}{(h_1-h_2)^2(6A-h_1+h_2)}(-6AF_0(h_1-h_2) + (h_1^3+h_2^3) \\ & - 6F_0h_1h_2 - 3h_1h_2(h_1-h_2))y + \frac{12(F_0+h_1-h_2)}{(h_1-h_2)^2(6A-h_1+h_2)}\frac{y^3}{3!},\end{aligned} \tag{37}$$

where

$$A = \beta(1-n).$$

The axial pressure gradient at this order is

$$\frac{dP_0}{dx} = \frac{12(1-n)(F_0+h_1-h_2)}{(h_1-h_2)^2(6A-h_1+h_2)}. \tag{38}$$

For one wavelength the integration of Eq. (38), yields

$$\Delta P_0 = \int_0^1 \frac{dP_0}{dx}dx. \tag{39}$$

3.4. Solution for System of Order We[1]

Substituting the zeroth-order solution (37) into (33), the solution of the resulting problem satisfying the boundary conditions take the following form

$$\Psi_1 = C_7 + C_6y + C_5\frac{y^2}{2!} + C_4\frac{y^3}{3!} + BC_3^2\frac{y^4}{4!}, \tag{40}$$

where

$$C_4 = \frac{12}{(h_1-h_2)^2(6A-h_1+h_2)^2}(F_1(h_1-h_2)^2(6A-h_1+h_2)-6B(F_0+h_1-h_2)^2(h_1+h_2)),$$

$$C_5 = \frac{1}{(h_1-h_2)^4(6A-h_1+h_2)^2(-2A+h_1-h_2)}(72A_1(h_1-h_2)^2(F_0+h_1-h_2)^2+6F_1(h_1-h_2)^2(2A-h_1+h_2)$$
$$\times(6A-h_1+h_2)(h_1+h_2)+12B(F_0+h_1-h_2)^2(h_1^3+3h_1^2h_2-h_2^3-3h_1h_2(4A+h_2))),$$

$$C_5 = \frac{1}{(h_1-h_2)^4(6A-h_1+h_2)^2(-2A+h_1-h_2)}(-72A^3F_1(h_1-h_2)^3-12A_1(h_1-h_2)^2(F_0+h_1-h_2)^2(h_1+h_2)$$
$$+24A^2F_1(h_1-h_2)^2(2h_1^2-7h_1h_2+2h_2^2)-6F_1(h_1-h_2)^3(h_1h_2(h_1-h_2)+A(h_1^2-10h_1h_2+h_2^2))$$
$$-12B(F_0+h_1-h_2)^2(h_1+h_2)(h_1h_2(h_1-h_2)+(h_1^2-4h_1h_2+h_2^2))),$$

$$C_7 = \frac{1}{2(h_1-h_2)^4(6A-h_1+h_2)^2(-2A+h_1-h_2)}(72A^2F_1(h_1+h_2)(h_1-h_2)^3-12A^2F_1(h_1+h_2)(h_1-h_2)^2$$
$$\times(5h_1^2-12h_1h_2+5h_2^2)-(h_1-h_2)(-12h_1h_2(F_0+h_1-h_2)^2(6A_1h_1-6A_1h_2+Bh_1h_2))$$
$$-(h_1-h_2)F_1(h_1-h_2)^3(h_1+h_2)(h_1^2-4h_1h_2+h_2^2)+24ABh_1h_2(F_0+h_1-h_2)^2(h_1^2-3h_1h_2+h_2^2)$$
$$+2F_1A(h_1-h_2)^3(h_1+h_2)(7h_1^2-22h_1h_2+7h_2^2)),$$

$$B = \frac{2n}{n-1}, \quad A_1 = \beta n.$$

The axial pressure gradient at this order is

$$\frac{dP_1}{dx} = \frac{12(1-n)}{(h_1-h_2)^4(6A-h_1+h_2)^2}(F_1(h_1-h_2)^2(6A-h_1+h_2)-6B(6A-h_1+h_2)^2(h_1+h_2))$$
$$+\frac{144n(F_0+h_1-h_2)^2(h_1+h_2)}{(h_1-h_2)^4(6A-h_1+h_2)(-6A+h_1-h_2)}. \tag{41}$$

For one wavelength the integration of Eq. (41), yields

$$\Delta P_1 = \int_0^1 \frac{dP_1}{dx}dx. \tag{42}$$

Summarizing the perturbation results for small parameter *We*, the expression for stream functions and pressure gradient can be written as

$$\psi = \frac{-1}{2(h_1-h_2)^2(-6A+h_1-h_2)}(-6AF_0(h_1^2-h_2^2)+F(h_1^3+h_2^3)-3Fh_1h_2(h_1+h_2)-2h_1h_2(h_1^2+h_2^2))$$
$$+\frac{6(F+h_1-h_2)(h_1+h_2)}{(h_1-h_2)^2(-6A+h_1-h_2)}\frac{y^2}{2!}+\frac{-1}{(h_1-h_2)^2(6A-h_1+h_2)}(-6AF(h_1-h_2)+(h_1^3+h_2^3) \tag{43}$$
$$-6Fh_1h_2-3h_1h_2(h_1-h_2))y+\frac{12(F+h_1-h_2)}{(h_1-h_2)^2(6A-h_1+h_2)}\frac{y^3}{3!}+We\left(C_7'+C_6'y+C_5'\frac{y^2}{2!}+C_4'\frac{y^3}{3!}+BC_3'^2\frac{y^4}{4!}\right),$$

where

$$C_3' = \frac{12(F+h_1-h_2)}{(h_1-h_2)^2(6A-h_1+h_2)},$$

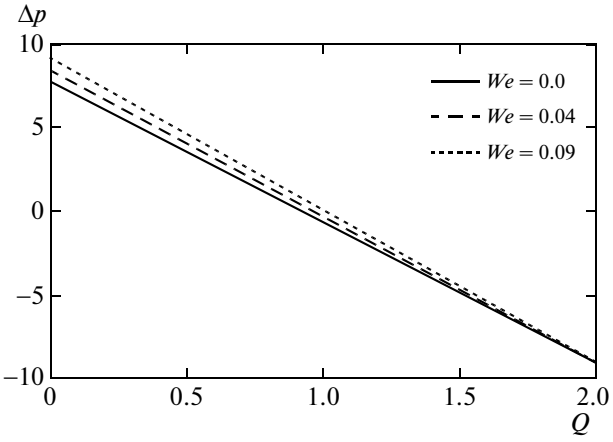

Fig. 1. Variation of ΔP with Q for different values of We. The other parameters are $a = 0.7$, $b = 0.5$, $d = 0.9$, $\phi = \pi/6$, $n = 0.06$, $\beta = 0.04$.

$$C_4' = \frac{12}{(h_1 - h_2)^2(6A - h_1 + h_2)^2}(-6B(F + h_1 - h_2)^2(h_1 + h_2)),$$

$$C_5' = \frac{1}{(h_1 - h_2)^4(6A - h_1 + h_2)^2(-2A + h_1 - h_2)}(72A_1(h_1 - h_2)^2(F + h_1 - h_2)^2$$
$$+ 12B(F + h_1 - h_2)^2(h_1^3 + 3h_1^2h_2 - h_2^3 - 3h_1h_2(4A + h_2))),$$

$$C_6' = \frac{1}{(h_1 - h_2)^4(6A - h_1 + h_2)^2(-2A + h_1 - h_2)}(-12A_1(h_1 - h_2)^2(F + h_1 - h_2)^2(h_1 + h_2)$$
$$- 12B(F + h_1 - h_2)^2(h_1 + h_2)(h_1h_2(h_1 - h_2) + (h_1^2 - 4h_1h_2 + h_2^2))),$$

$$C_7' = \frac{1}{2(h_1 - h_2)^4(6A - h_1 + h_2)^2(-2A + h_1 - h_2)}(12h_1h_2(h_1 - h_2)(F + h_1 - h_2)^2(6A_1h_1 - 6A_1h_2 + Bh_1h_2)$$
$$+ 24ABh_1h_2(F + h_1 - h_2)^2(h_1^2 - 3h_1h_2 + h_2^2)),$$

$$\frac{dP}{dx} = \frac{12(1-n)(F + h_1 - h_2)}{(h_1 - h_2)^2(6A - h_1 + h_2)} + We\left(\frac{-72(1-n)B(F + h_1 - h_2)^2(h_1 + h_2)}{(h_1 - h_2)^4(6A - h_1 + h_2)^2}\right.$$
$$\left. + \frac{144n(F + h_1 - h_2)^2(h_1 + h_2)}{(h_1 - h_2)^4(6A - h_1 + h_2)(-6A + h_1 - h_2)}\right). \quad (44)$$

The non-dimensional pressure rise over one wavelength ΔP is defined as

$$\Delta P = \int_0^1 \frac{dP}{dx}dx, \quad (45)$$

where dP/dx is defined in Eq. (44).

4. RESULTS AND DISCUSSION

In this section the graphical results are displayed to see the effects of various physical parameters on the pressure rise, pressure gradient, velocity profile and streamlines. The expression for the pressure rise over one wave length is calculated numerically using Mathematics software. Figures 1 to 6 are plotted for pressure rise against the volume flow rate Q. It is observed that the relation between the pressure rise and the

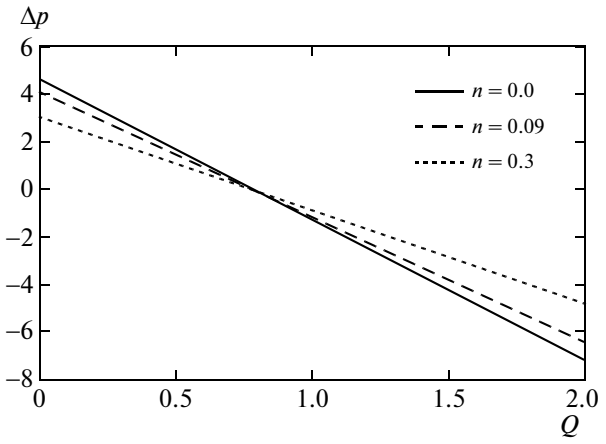

Fig. 2. Variation of ΔP with Q for different values of n. The other parameters are $a = 0.6$, $b = 0.5$, $d = 0.9$, $\phi = \pi/6$, $We = 0.06$, $\beta = 0.02$.

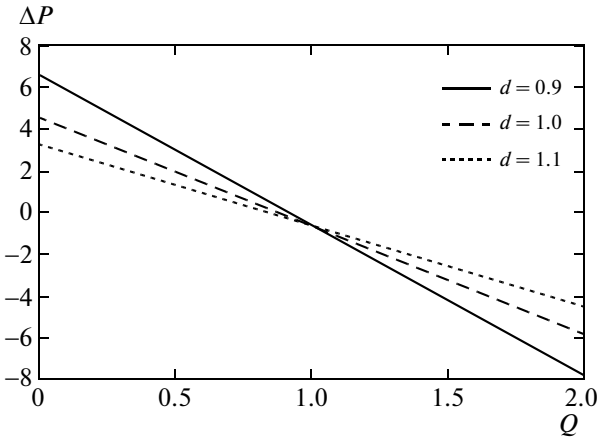

Fig. 3. Variation of ΔP with Q for different values of d. The other parameters are $a = 0.5$, $b = 0.5$, $We = 0.04$, $\phi = \pi/6$, $n = 0.06$, $\beta = 0.02$.

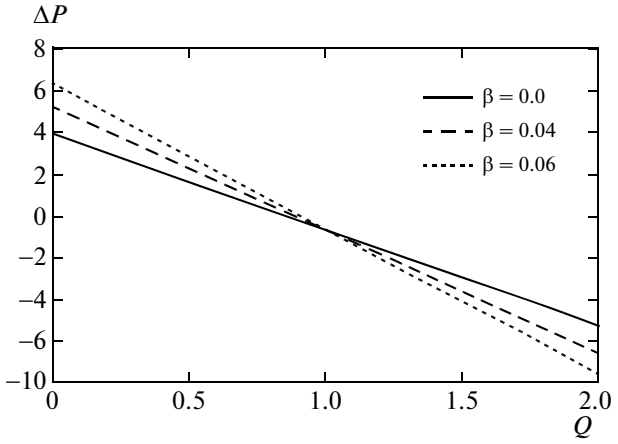

Fig. 4. Variation of ΔP with Q for different values of β. The other parameters are $a = 0.7$, $b = 0.5$, $d = 1$, $\phi = \pi/6$, $n = 0.06$, $We = 0.04$.

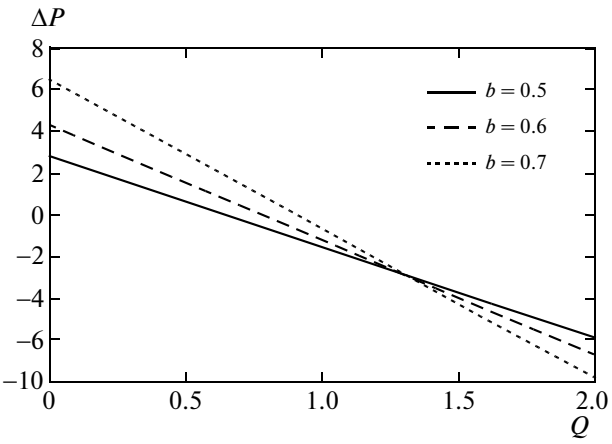

Fig. 5. Variation of ΔP with Q for different values of b. The other parameters are $a = 0.5$, $We = 0.04$, $d = 0.9$, $\phi = \pi/6$, $n = 0.04$, $\beta = 0.02$.

volume flow rate is inversely proportional to each other. In Fig. 1 it is observed that in the pumping region ($\Delta P > 0$) the pressure rise increases with the increase in Weissenberg number We. It is also observed from Figs. 2 and 3, that the pressure rise decreases with the increase of power law index n and the width of the channel d in the pumping ($\Delta P > 0$) and free pumping ($\Delta P = 0$) region while in the copumping ($\Delta P < 0$) region the pressure rise increases with the increase in n and d. It is also depicted from Figs. 4 to 6 that in the pumping ($\Delta P > 0$) and free pumping ($\Delta P = 0$) region the pressure rise increases with the increase in the slip parameter β, and the amplitudes of the wave a and b, while the behavior is opposite in the copumping ($\Delta P < 0$) region. The pressure gradient for different values of β, n and a are prepared in Figs. 7 to 9. It is observed that the magnitude of pressure gradient increases with the increase in β and decreases with the increase in n (see Figs. 7 and 8). However, with the increase in a the magnitude of pressure gradient decreases in the region $x \in [0, 0.2]$ and $[0.8, 1]$, where as in the region $x \in [0.2, 0.8]$ it is increases. The velocity profiles for the different values of Weissenberg number We, volume flow rate Q, and slip parameter β are shown in Figs. 10 to 12. It is observed from Fig. 10 that the magnitude value of the velocity field increases with the increase in Weissenberg number We. From Fig. 11 it is shown that the magnitude value of the velocity field decreases with the increase in the volume flow rate Q. It is depicted from Fig. 12 that due to the slip parameter β the velocity near the channel walls is not the same but it is sliding and also the velocity increases with the increase in β.

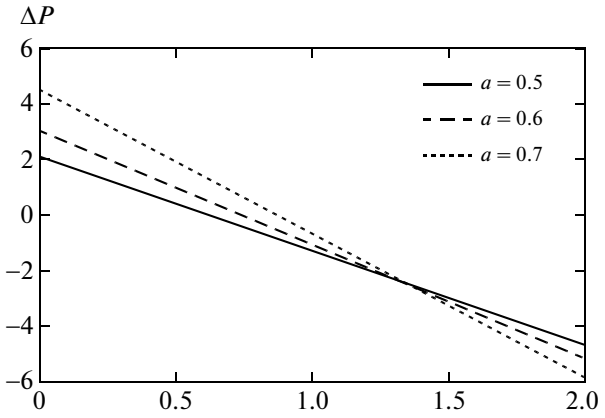

Fig. 6. Variation of ΔP with Q for different values of a. The other parameters are $We = 0.04$, $b = 0.5$, $d = 1$, $\phi = \pi/6$, $n = 0.06$, $\beta = 0.02$.

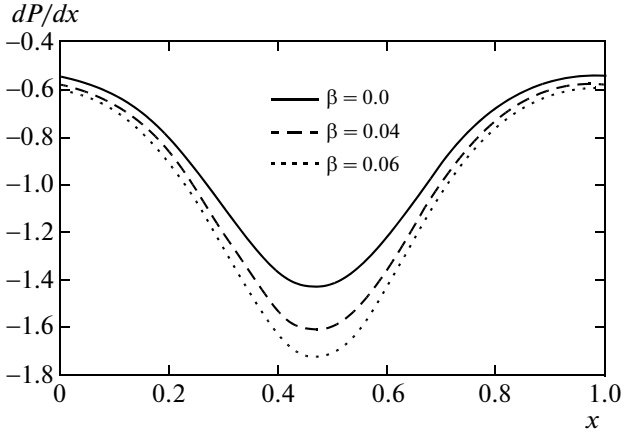

Fig. 7. Variation of dP/dx with x for different values of β. The other parameters are $a = 0.5$, $b = 0.5$, $d = 2$, $\phi = \pi/8$, $Q = 2$, $n = 0.04$, $We = 0.04$.

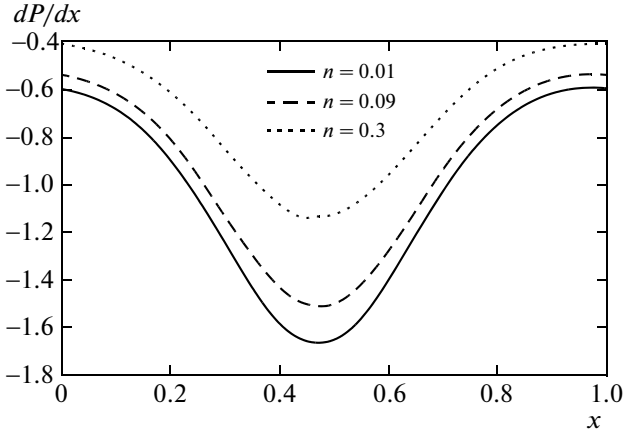

Fig. 8. Variation of dP/dx with x for different values of n. The other parameters are $a = 0.5$, $b = 0.5$, $d = 2$, $\phi = \pi/8$, $Q = 2$, $We = 0.04$, $\beta = 0.04$.

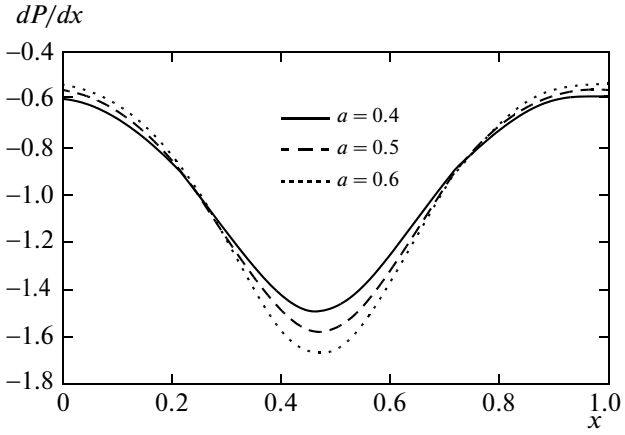

Fig. 9. Variation of dP/dx with x for different values of a. The other parameters are $We = 0.04$, $b = 0.5$, $d = 2$, $\phi = \pi/8$, $Q = 2$, $n = 0.06$, $\beta = 0.04$.

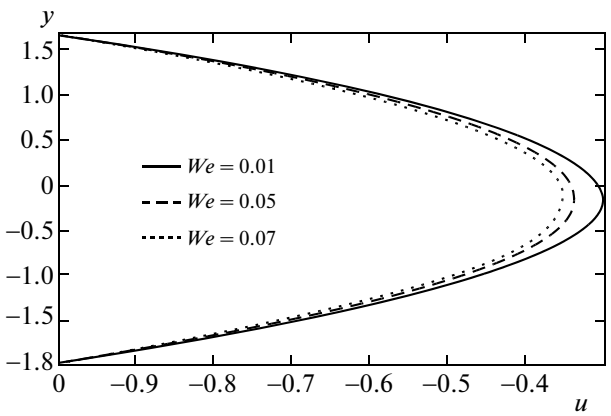

Fig. 10. Velocity profile for different values of We. The other parameters are $a = 0.7$, $b = 1.2$, $d = 2$, $\phi = \pi/2$, $Q = 1$, $n = 0.3$, $\beta = 0.06$.

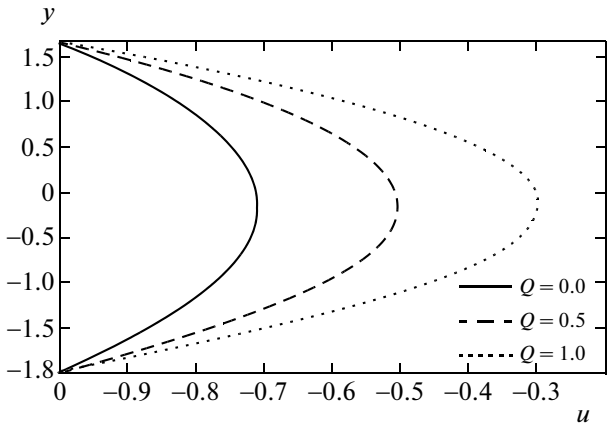

Fig. 11. Velocity profile for different values of Q. The other parameters are $a = 0.7$, $b = 1.2$, $d = 2$, $\phi = \pi/2$, $We = 0.06$, $n = 0.4$, $\beta = 0.06$.

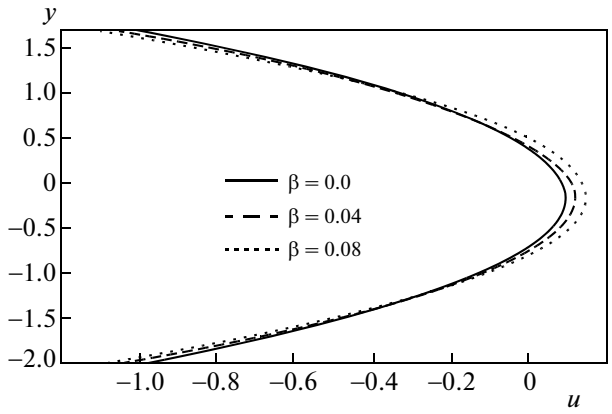

Fig. 12. Velocity profile for different values of β. The other parameters are $a = 0.7$, $b = 1.2$, $d = 2$, $\phi = \pi/2$, $Q = 2$, $n = 0.04$, $We = 0.06$.

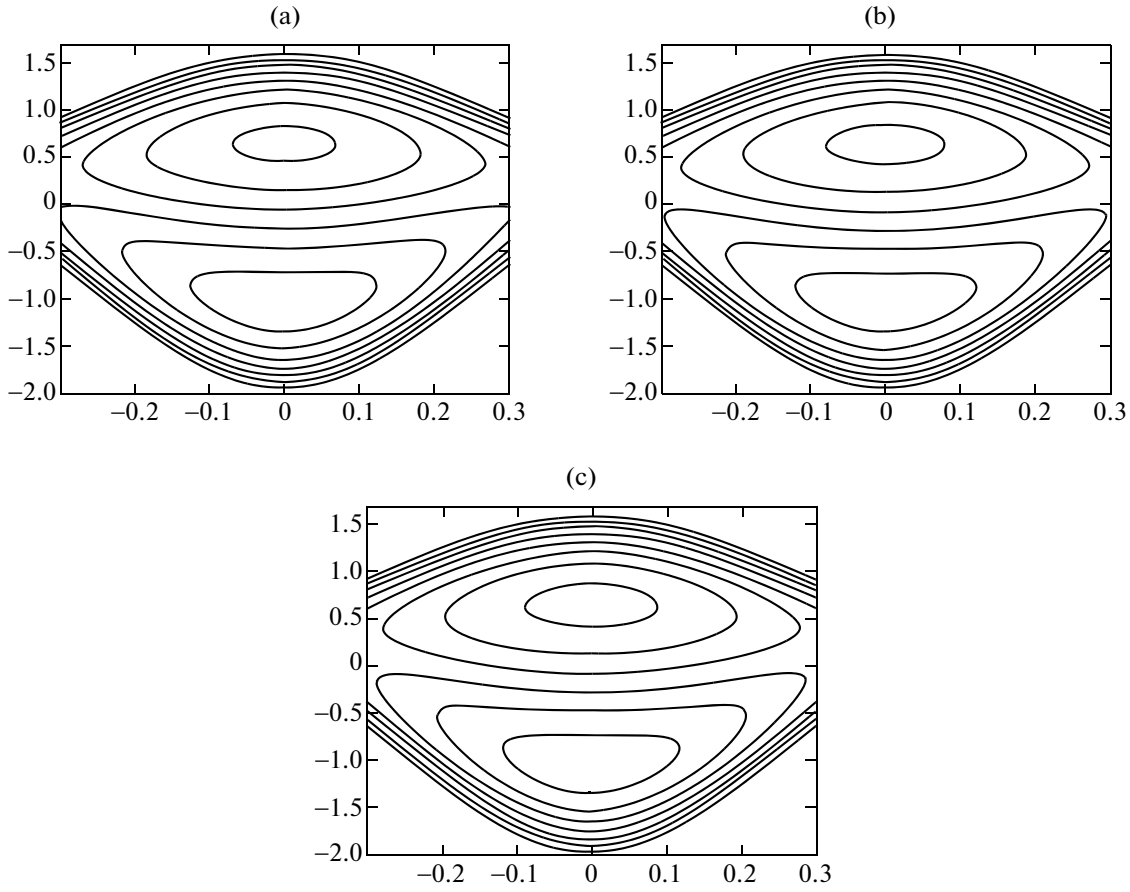

Fig. 13. Stream lines for different values of *We*. (a) for $We = 0.01$, (b) for $We = 0.05$ and (c) for $We = 0.07$. The other parameters are $\phi = 0.01$, $Q = 1.5$, $a = 0.5$, $n = 0.04$, $d = 0.9$, $b = 1.0$, $\beta = 0.02$.

The trapping phenomena for the different values of Weissenberg number *We*, power law index *n*, slip parameter β and volume flow rate *Q* are shown in Figs. 13 to 16. It is seen from Fig. 13 and 14 that the size of the trapping bolus increases with the increase of the Weissenberg number *We* and power law index *n* in the upper half of the channel, while in the lower half the size of the bolus decreases. From Fig. 15 it is observed that with the increase of slip parameter ft the size of the trapping bolus increases in lower and

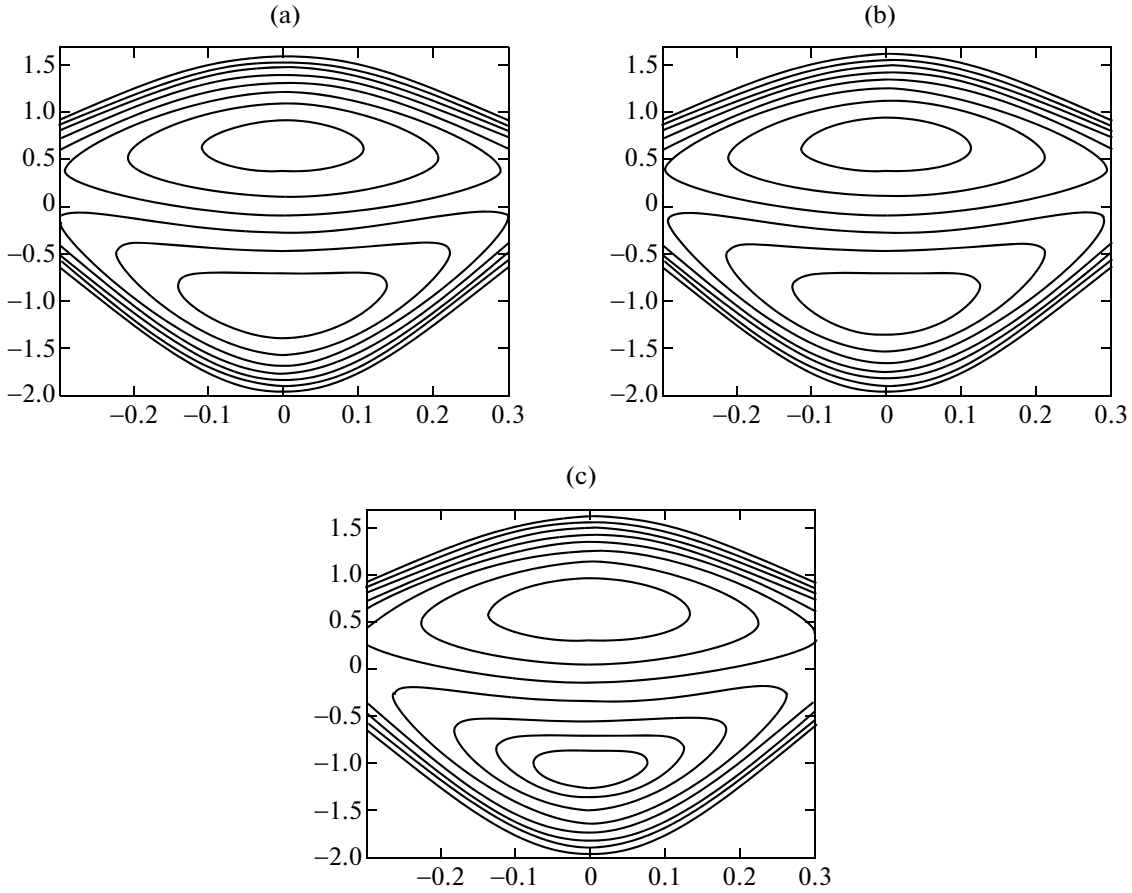

Fig. 14. Stream lines for different values of n. (a) for $n = 0.01$, (b) for $n = 0.09$ and (c) for $n = 0.3$. The other parameters are $\phi = 0.01$, $Q = 1.5$, $a = 0.5$, $We = 0.06$, $d = 0.9$, $b = 1.0$, $\beta = 0.06$.

upper halves of the channel. It is also observed from Fig. 16 that with the increase in Q, the size of the trapped bolus decreases in the upper half of the channel, while in the lower half the behavior is quite opposite, here size of the trapping bolus increases.

Table 1 and 2 shows the comparsion of the present work with Nadem and Akram [22].

Table 1. Comparsion of the velocity profile for fixed $Q = 1$, $a = 1$, $b = 1.2$, $d = 2$, $\phi = \pi/2$, $x = 1$, $n = 0.4$, $We = 0.06$

y	$u(x, y)$ for present work when $\beta = 0.06$	$u(x, y)$ for Nadeem et al. [22] when $b = 0.0$
−2	−1	−1
−1.6	−0.748365	−0.734475
−1.2	−0.527891	−0.525883
−0.8	−0.368432	−0.375135
−0.4	−0.270793	−0.28295
0	−0.235779	−0.250049
0.4	−0.264193	−0.277152
0.8	−0.356841	−0.364978
1.2	−0.514528	−0.514248
1.6	−0.738057	−0.725682
2	−1	−1

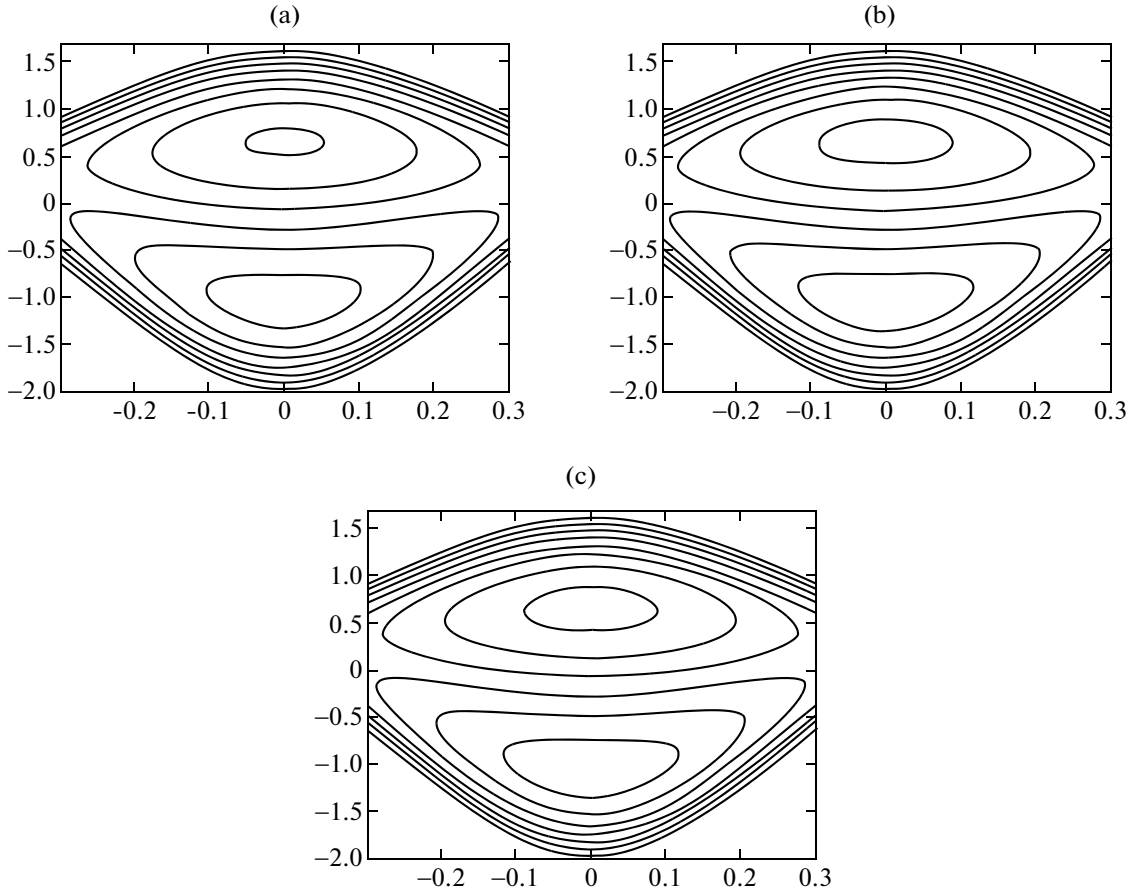

Fig. 15. Stream lines for different values of β. (a) for $\beta = 0.02$, (b) for $\beta = 0.04$ and (c) for $\beta = 0.06$. The other parameters are $\phi = 0.01$, $Q = 1.5$, $a = 0.5$, $We = 0.09$, $d = 0.09$, $b = 1.0$, $n = 0.04$.

4.1. Concluding Remarks

In this paper we have investigated the slip effects on the peristaltic flow of tangent hyperbolic fluid in an asymmetric channel. The governing two dimensional equations have been modeled and then simplified under the long wave length and low Reynolds number approximation. The simplified equations are solved analytically using the regular perturbation method. The results are discussed through graphs. We conclude the following remarks:

Table 2. Comparsion of the variation of ΔP for fixed $a = 0.7$, $b = 0.5$, $d = 1$, $\phi = \pi/6$, $n = 0.06$, $We = 0.04$

y	ΔP for present work when $\beta = 0.04$	ΔP for Nadeem et al. [22] when $\beta = 0.0$
0	5.26525	3.97069
0.2	4.0836	3.05179
0.4	2.90196	2.13289
0.6	1.72031	2.13289
0.8	0.538667	0.295092
1.0	−0.42978	−0.623808
1.2	−1.82462	−1.54271
1.4	−3.00627	−2.46161
1.6	−4.18791	−2.46161
1.8	−5.36956	−4.29941
2.0	−6.5512	−5.21831

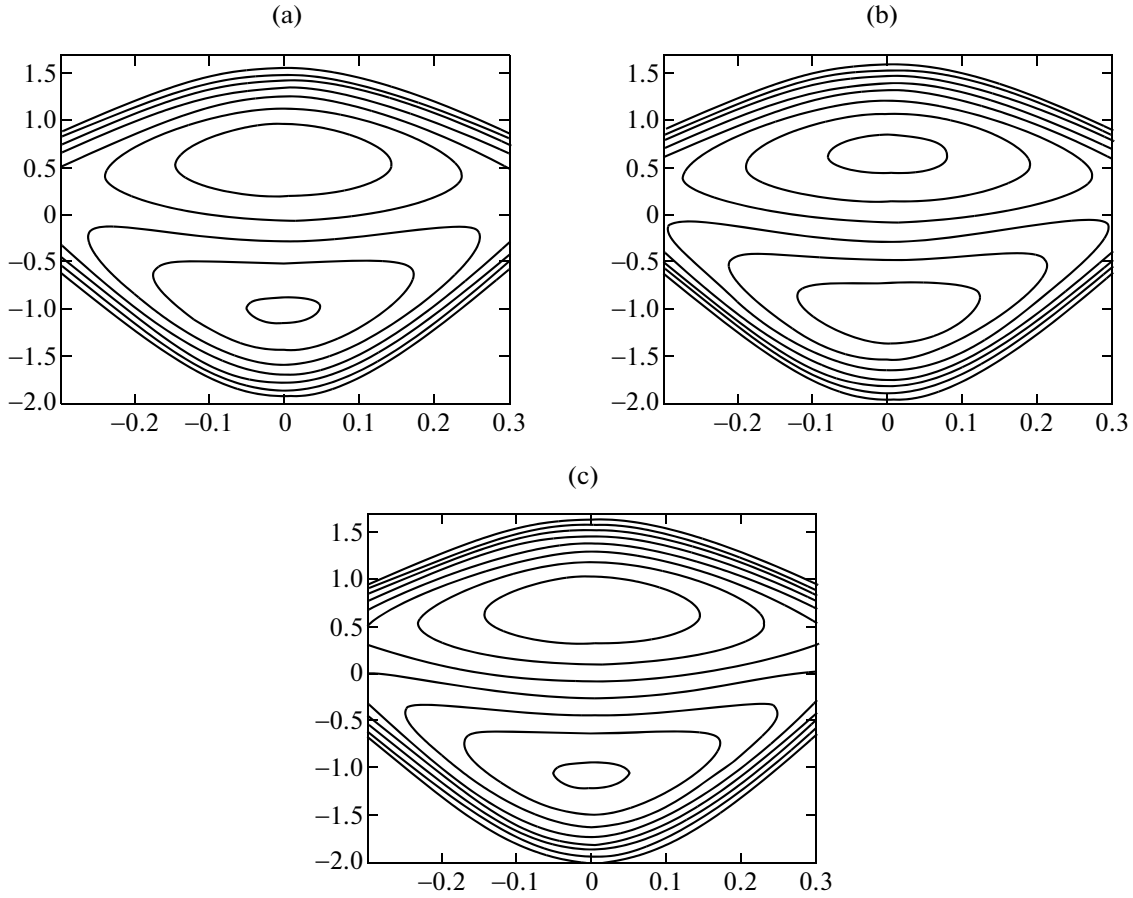

Fig. 16. Stream lines for different values of Q. (a) for $Q = 1.4$, (b) for $Q = 1.5$ and (c) for $Q = 1.6$. The other parameters are $\phi = 0.01$, $\beta = 0.04$, $a = 0.5$, $We = 0.06$, $d = 0.9$, $b = 1.0$, $n = 0.02$.

1. It is observed that in the peristaltic pumping region ($\Delta P > 0$) the pressure rise increases with an increase in We, β, a and b.

2. It is also observed that the pressure rise decreases with the increase of power law index n and width of the channel d in the pumping ($\Delta P > 0$) and free pumping ($\Delta P = 0$) regions, while in the copumping ($\Delta P < 0$) region the pressure rise increases with an increase in n and d.

3. The pressure gradient increases with an increase in both β and a, while it decreases with an increase in n.

4. It is observed that the velocity field increases with an increase in Weissenberg number We and decreases with an increase in the volume flow rate Q.

5. It is also observed that due to slip parameter β the velocity near the channel walls is not same. Moreover the velocity increases with an increase in β.

6. The size of the trapping bolus increases in the upper half of the channel and decreases in the lower half of the channel with an increase of We and n, while the behavior is opposite in the case when the volume flow rate Q increases.

7. With an increase of the slip parameter β the size of the trapping bolus increases.

REFERENCES

1. T. D. Brown and T. K. Hung, "Computational and experimental investigations of two dimensional non linear peristaltic flows," J. Fluid Mech. **83**, 249–272 (1977).

2. S. Nadeem and Safia Akram, "Peristaltic flow of a Williamson fluid in an asymmetric channel," Commun. Nonlinear Sci. Numer. Simul. doi : 10.1016/j.cnsns.2009.07.026.

3. Safia Akram and S. Nadeem, "Influence of induced magnetic field and heat transfer on the peristaltic motion of a Jeffrey fluid in an asymmetric channel: Closed form solutions," J. Magn. Magn. Mater. **328**, 11–20 (2013).
4. Safia Akram, S. Nadeem, and M. Hanif, "Numerical and analytical treatment on peristaltic flow of Williamson fluid in the occurrence of induced magnetic field," J. Magn. Magn. Mater. **346**, 142–151 (2013).
5. Kh. S. Mekheimer and Y. Abd elmaboud, "The influence of heat transfer and magnetic field on peristaltic transport of a Newtonian fluid in a vertical annulus: Application of an endoscope," Phys. Lett. A **372**, 1657–1665 (2008).
6. T. Hayat and N. Ali, "Peristaltically induced motion of a MHD third grade fluid in a deformable tube", Physica A **370**, 225–239 (2006).
7. S. Nadeem, Safia Akram, and Noreen Sher Akbar, "Simulation of heat and chemical reactions on peristaltic flow of a Williamson fluid in an inclined asymmetric channel," Iran. J. Chem. Chem. Eng. **32**, 93–107 (2013).
8. Kh. S. Mekheimer, "Effect of the induced magnetic field on peristaltic flow of a couple stress fluid," Phys. Lett. A **372**, 4271–4278 (2008).
9. A. H. Shapiro, M. Y. Jaffrin, and S. L. Weinberg, "Peristaltic pumping with long wave length at low Reynolds number," J. Fluid Mech. **37**, 799–825 (1969).
10. T. W. Latham, M. Sci. Thesis (Massachusetts Institute of Technology, Cambridge, 1966).
11. Safia Akram and S. Nadeem, "Significance of nanofluid and partial slip on the peristaltic transport of a Jeffrey fluid model in an asymmetric channel with different wave forms," IEEE Trans. Nanotech. **13**, 375–385 (2014).
12. M. Mishra and A. R. Rao, "Peristaltic transport of a Newtonian fluid in an asymmetric channel," Z. Angew. Math. Phys. **54**, 532–550 (2004).
13. Safia Akram, Kh.S. Mekheimer, and S. Nadeem, "Influence of lateral walls on peristaltic flow of a couple stress fluid in a non-uniform rectangular due," Appl. Math. Inf. Sci **3**, 1127–1133 (2014).
14. M. H. Haroun, "Effect of Deborah number and phase difference on peristaltic transport in an asymmetric channel," Commun. Nonlinear Sci. Numer. Simul. **12**, 1464–1480 (2007).
15. Safia Akram and S. Nadeem, "Consequence of nanofluid on Peristaltic transport of a hyperbolic Tangent fluid model in the occurrence of apt (tending) magnetic field," J. Magn. Magn. Mater. **358–359**, 183–191 (2014).
16. G. Radhakrishnamacharya and Ch. Srinivasulu, "Influence of wall properties on peristaltic transport with heat transfer" C. R. Mecanique **335**, 369–373 (2007).
17. T. Hayat, Q. Hussain, and N. Ali, "Influence of partial slip on the peristaltic flow in a porous medium," Physica A **387**, 3399–3409 (2008).
18. A. Ebaid, "Effects of magnetic field and wall slip conditions on the peristaltic transport of a Newtonian fluid in an asymmetric channel," Phys. Lett. A **372**, 4493–4489 (2008).
19. T. Hayat, M. Umar Qureshi, and N. Ali, "The influence of slip on the peristaltic motion of a third order fluid in an asymmetric channel," Phys. Lett. A **372**, 2653–2664 (2008).
20. S. Nadeem and Safia Akram, "Slip effects on the peristaltic flow of a Jeffrey fluid in an asymmetric channel under the effect of induced magnetic field," Int. J. Numer. Methods Fluids doi: 10.1002/fld.2081.
21. L. Ai and K. Vafai, "An investigation of Stokes second problem for non-Newtonian fluids," Numer. Heat Transfer, Part A **47**, 955–980 (2005).
22. S. Nadeem and Safia Akram, "Peristaltic transport of a hyperbolic tangent fluid model in an asymmetric channel," Z. Naturforschung A **64**, 559–567 (2009).